

Biochemistry. Author manuscript; available in PMC 2012 March 1.

Published in final edited form as:

Biochemistry. 2011 March 1; 50(8): 1359–1367. doi:10.1021/bi101749s.

# The Cullin-RING E3 ubiquitin ligase CRL4-DCAF1 complex dimerizes via a short helical region in DCAF1

Jinwoo Ahn $^{1,2,*}$ , Zach Novince $^{1,2}$ , Jason Concel $^{1,2}$ , Chang-Hyeock Byeon $^{1,2}$ , Alexander M. Makhov $^2$ , In-Ja L. Byeon $^{1,2}$ , Peijun Zhang $^{1,2}$ , and Angela M. Gronenborn $^{1,2,*}$ 

- <sup>1</sup> University of Pittsburgh Center for HIV Protein Interactions, University of Pittsburgh School of Medicine, Pittsburgh, PA 15260 USA
- <sup>2</sup> Department of Structural Biology, University of Pittsburgh School of Medicine, Pittsburgh, PA 15260 USA

#### Abstract

The cullin4A-RING E3 ubiquitin ligase (CRL4) is a multisubunit protein complex, comprising cullin4A (CUL4), RING H2 finger protein (RBX1) and DNA damage-binding protein 1 (DDB1). Proteins that recruit specific targets to CRL4 for ubiquitination (ubiquitylation), bind the DDB1 adaptor protein via WD40 domains. Such CRL4 substrate recognition modules are DDB1- and CUL4-associated factors (DCAFs). Here we show that for DCAF1, oligomerization of the protein and the CRL4 complex occurs via a short helical region (residues 845–873) N-terminal to DACF1's own WD40 domain. This sequence was previously designated as a LIS1 homology (LisH) motif. The oligomerization helix contains a stretch of four Leu residues, which appear to be essential for alpha-helical structure and oligomerization. *In vitro* reconstituted CRL4-DCAF1 complexes (CRL4<sup>DCAF1</sup>) form symmetric dimers as visualized by electron microscopy (EM) and dimeric CRL4<sup>DCAF1</sup> is a better E3 ligase for *in vitro* ubiquitination of the UNG2 substrate compared to a monomeric complex.

Protein degradation is a highly regulated process carried out by the ubiquitin-proteasome system (1-3). It involves covalent modification of protein substrates with multiple copies of ubiquitin (Ub) chains, followed by proteolysis of the Ub-tagged proteins by the 26S proteasome (4,5). Post-translational ubiquitination is extremely diverse, variable in multimer length and linkage type. While attachment of a single Ub module affects protein localization (6), poly-ubiquitination at different Lys residues of Ub targets proteins for degradation or regulation of activity (7–9). Ub-modification involves a concerted series of enzymatic reactions. The first enzyme, E1, activates Ub in an Mg-ATP dependent manner, creating a covalent thiolester-linked E1~Ub complex (Ub(T)) with a second Ub bound at the adenylation active site (Ub(A)). Subsequently, the thiolester-linked Ub(T) is transferred to a reactive Cys on a cognate E2 conjugating enzyme by trans-esterification, and Ub-loaded E2s are released from E1s for substrate attachment by E3s (10-12). Two different classes of E3 ligases have been characterized that either contain a HECT (homologous to E6-AP Cterminus) or a RING (Really Interesting New Gene) domain. The RING domain protein, RBX1 forms modular complexes with several homologous cullin scaffold subunits (CUL1 to CUL7; reviewed in (13)). Each CUL-RBX1 heterodimer uses a specific adaptor protein to form a multi-subunit complex, referred to as a cullin-RING ubiquitin ligase (CRL1-7). The RING domain mainly functions as a docking site for the E2 enzyme (14–16) at the C-

<sup>\*</sup>Correspondence should be addressed to: Jinwoo Ahn, 3501 Fifth Avenue, Pittsburgh, PA 15260 USA, Tel: 412-383-6933, Fax: 412-648-9008, jia12@pitt.edu. Angela M. Gronenborn, 3501 Fifth Avenue, Pittsburgh, PA 15260 USA, Tel: 412-648-9959, Fax: 412-648-9008, amg100@pitt.edu.

terminus of the cullin, while the adaptor proteins bind to the N-terminus of the cullin and position substrate receptors and target proteins for ubiquitination (13,17,18). One of the adaptor proteins is DDB1 (DNA damage-binding protein 1), a 127 kDa modular protein that contains three seven-bladed  $\beta$ -propeller WD40 domains (19–21). DDB1 specifically associates with CUL4 and binds more than 50 different DCAFs (DDB1-and CUL4-associated factors) that function as substrate receptor proteins (22–25). DCAF proteins also contain a WD40 domain that is used for interacting with DDB1(21,24–26).

For most DCAF proteins, neither cellular function nor targets have been identified. Those cellular targets that have been identified were shown to function in chromatin re-modeling, DNA replication, cell cycle regulation, and apoptosis (27,28). Intriguingly, Vpr, one of the four accessory proteins encoded by HIV-1, interacts with DCAF1, possibly targeting unidentified cellular factors for degradation, and mediating Vpr's biological activity in G2/M-phase cell-cycle arrest (29–37)

It has been argued that in CRL-substrate receptor complexes, differences in substrates sizes may present a problem for poly-ubiquitination given the variable distance between the catalytic site on E2 and the target Lys residue(s) on the substrate. If present, structural constraints imposed by the rigid cullin scaffold in CRLs can be resolved by positioning a flexible hinge somewhere in the complex. This appears to be the achieved by NEDD8 modification at the C-terminus of CUL, shown to impart conformational flexibility onto CUL and RBX1, thereby facilitating poly-ubiquitination of the substrates (38,39). An alternative mechanism could exploit dimerization and, indeed, for several CRLs, dimerization via the substrate receptor proteins has been reported (reviewed in (18)). Dimerization allows for poly-ubiquitination *in trans* as well as *in cis* without affecting the substrate affinity (40–44).

Here, we report that DCAF1 can oligomerize through an alpha helical region that was originally identified as a LisH motif. This region is located N-terminal to the WD40 domain, although quite distant with ca. 200 residues separating the two regions. *In vitro* biochemical studies and electron microscopy of CRL4<sup>DCAF1</sup> complexes reveal that the E3 ubiquitin ligase indeed forms an oligomeric supramolecular complex that could aid to accommodate a variety of substrate sizes for ubiquitination.

#### **Experimental Procedures**

#### **Cloning and Construction of Plasmids**

The cDNA for DCAF1 was purchased from Open Biosystems and codes for residues 97–1507. DCAF1 constructs comprising amino acids 572–1507, 817–1507, 876–1396, 987–1396, and 1005–1507 were cloned into the pIZ/V5-His vectors (Invitrogen), resulting in His<sub>6</sub>- and V5-tags at the C-termini of the protein constructs. In addition, N-terminally FLAG-tagged or Myc-tagged DCAF1 constructs, encoding residues 96–1507 were cloned into pIZ/V5-His vectors, respectively. Site-directed mutagenesis was carried out on pIZ/V5-His DCAF1 817–1507 using QuickChange kits (Stratagene) to create the L850E/L851E and L852E/L853 mutants. Constructs coding for residues 809–876 were amplified from the pIZ/V5-His DCAF1 817–1507 WT DNA and the two mutants, and cloned into pET32 vectors (Invitrogen). Other DCAF1 constructs coding for residues 809–902 and 841–883 were also cloned into the pET32 vectors. The pET32 vectors were modified to contain a TEV protease recognition site between the thioredoxin fusion partner and the target protein (45). For baculoviruses expressing DCAF1 proteins, constructs coding for 817–1507, 987–1396 and 1005–1507 were cloned into the pENT vector (Invitrogen). Recombinant baculoviruses expressing C-terminally His<sub>6</sub>-tagged DCAF1 proteins were prepared using Baculodirect C-

term (Invitrogen) and pENT-DCAF1 vectors, according to the manufacturer's protocol. Nucleotide sequences were verified for the entire coding regions of all constructs.

#### **Expression and Purification of Proteins**

Thioredoxin(pET32)-tagged DCAF1 809-876 WT, L850E/L851E, L852E/L853E mutant, DCAF1 809–902, and 841–883 constructs containing His<sub>6</sub>- tag between thioredoxin and the TEV protease recognition site were expressed in E. coli Rosetta 2 (DE3), cultured in Luria-Bertani media, using 0.4 mM IPTG for induction and growth at 18 °C for 16 h. The DCAF1 809-876 WT, L850E/L851E, L852E/L853E mutant constructs contain an additional Cterminal His<sub>6</sub>-tag. Uniform 13C/15N labeling of DCAF1 809–876 WT, DCAF1 809–902, and DCAF1 841-883 proteins was carried out by growth in modified medium using 15NH<sub>4</sub>Cl and/or 13C<sub>6</sub>-glucose as sole nitrogen and carbon sources, respectively. Soluble forms of His<sub>6</sub>-tagged proteins were purified using 5 mL Ni-NTA columns (GE Heatlthcare) and aggregated materials were removed by gel-filtration column chromatography using Hi-Load Superdex 200 16/60 column (GE Healthcare), equilibrated with a buffer containing 25 mM sodium phosphate, pH 7.5, 150 mM NaCl, 1 mM DTT, 10% glycerol, and 0.02% sodium azide. Thioredoxin-tagged DCAF1 proteins were digested with TEV protease, and DCAF1 proteins were purified over an 8 mL MONO Q column (GE Healthcare), equilibrated with 25 mM TrisHCl, pH 8.5, and 0.02% azide, using a 0-1 M NaCl gradient for elution. C-terminally His<sub>6</sub>- tagged DCAF1 817–1507, 1005–1507, and 987–1396 proteins were co-expressed with N-terminally His<sub>10</sub>- and FLAG-tagged DDB1 in SF21 insect cells (Invitrogen). The N-terminally His<sub>6</sub>-tagged RBX1 and CUL4A were also coexpressed in SF21 cells. Expression of proteins in insect cells and purification were performed as described previously (46). For preparation of multi-protein complexes composed of CUL4A, RBX1, DDB1, and DCAF1 proteins, all components were mixed at equimolar ratios and the protein complexes were purified over an 8 mL MONO Q column (GE Healthcare) at pH 7.5, using a 0-1 M NaCl gradient for elution. Purified complexes were analyzed by SDS-PAGE and native PAGE and visualized by Coomassie Blue staining. All other proteins used in this report were prepared as previously described (46).

#### **Insect Cell Cultures and Transient Transfection**

SF9 cells (Invitrogen) were cultured in SF-900 II SFM medium containing 2% fetal bovine serum. Cells were plated in 10 cm plates at 90% confluency 2 h prior to transient transfection. The cells were co-transfected with a total of 16  $\mu g$  pIZ/V5-His plasmids coding for the various DCAF1 constructs as indicated using Cellfectin II (Invitrogen), according to the manufacturer's protocol. Cells were harvested 48 h after transfection and subjected to immunoprecipitation as described below. *Immunoprecipitation and Immunoblotting*. Transiently transfected SF9 cells were harvested and treated with 400  $\mu L$  of a lysis buffer containing phosphate buffered saline (PBS), 5% glycerol, 1% Tween 20, 1% NP-40, 0.2 mM phenylmethylsulfony fluoride, and protease inhibitor cocktail (EMD Biosciences). The lysates were incubated with 40  $\mu L$  of anti-FLAG agarose affinity gel for 4 h, and the beads were washed four times with 500  $\mu L$  of the lysis buffer. Immunoprecipitates were eluted from the beads with 50  $\mu L$  of sample loading buffer or FLAG peptides at a concentration of 100  $\mu g/mL$ . Eluted proteins were separated by SDS-PAGE, and probed by immunoblotting. For detection of proteins, anti-Myc (Sigma), anti-FLAG (Sigma), and anti-V5 (Sigma) antibodies were used.

#### **NMR Spectroscopy**

All NMR experiments were recorded at 25 °C using a Bruker AVANCE600 spectrometer, equipped with a 5-mm triple-resonance, *z*-axis gradient cryoprobe, on samples containing 0.3mM  $^{13}$ C/ $^{15}$ N-labeled DCAF1 809–876, 809–902, and 841–883 peptides in 25mM sodium phosphate buffer, pH 6.5, 150 mM sodium chloride, 0.02% sodium azide. Backbone

and C $\beta$  resonance assignments of DCAF1 809–876, 809–902 and 841–883 were carried out using 2D  $^1H$ - $^{15}N$  HSQC and 3D HNCACB and HN(CO)CACB experiments. Secondary structure elements of these peptides were obtained based on secondary chemical shifts using  $\Delta C_{\alpha}$  minus  $\Delta C_{\beta}$  with  $\Delta C_{\alpha}$  and  $\Delta C_{\beta}$  values calculated by subtracting random coil  $C_{\alpha}$  and  $C_{\beta}$  shifts from the measured values (47,48).

#### **Multi-angle Light Scattering**

The molecular masses of protein complexes were obtained using an analytical Superdex200 column (1 cm  $\times$  30 cm, GE Healthcare) with in-line multi-angle light scattering (HELEOS, Wyatt Technology), variable wavelength UV (Agilent 1100 Series, Agilent Technology), and refractive index (Optilab rEX, Wyatt Technology) detection. Typically, about 100  $\mu$ L of 2 mg/mL of protein solutions were injected into the column that was pre-equilibrated with a buffer containing 25 mM sodium phosphate, pH 7.5, 150 mM NaCl, 5% glycerol, and 0.02% sodium azide at a flow rate of 0.5 mL/min at room temperature. Light scattering data were analyzed using the ASTRA program (Wyatt Technology).

#### Circular Dichroism (CD) Spectroscopy

Far-UV (195–250 nm) CD spectra of DCAF1 809–876 WT, L850E/L851E, and L852E/L853E mutants were recorded at a concentration of 3.3 μM in 2.5 mM sodium phosphate buffer, pH 7.5, 15 mM NaCl, at 25°C using a JASCO-810 (Easton, MD) spectrophotometer. Data were collected with 0.5 nm intervals and averaged 10 times. *Electron Microscopy (EM) Analysis*. The purified CRL4<sup>DCAF1</sup> complex composed of RBX1-CUL4A-DDB1-DCAF1 817–1507 at a concentration of 0.8 mg/ml was diluted 50 fold and deposited onto glow-discharged carbon foil grids, blotted with filter paper, and stained with 2% uranyl acetate. The grids were examined at 200 kV with a TF20 electron microscope (FEI, Hillsboro, OR). Images were recorded with a 4K×4K Gatan CCD camera (Gatan, Inc., Warrendale, PA) at a nominal magnification of 50,000x and underfocus values ranging from 1.5 to 3.0 μm.

#### **Image Processing of EM**

EM images were processed using the EMAN image analysis software (49). Individual particles were boxed manually with  $208 \times 208$  pixels (2.14 Å/pixel), normalized, and combined to yield one raw image stack file. A total of 1900 individual particle images was selected, band pass-filtered, and aligned with respect to their center of mass. The aligned raw projection images were classified using reference-free multi-variance statistical analysis and averaged within each class.

#### In Vitro Ubiquitination Assays

Typically, E1 (UBA1,  $0.2~\mu M$ ), E2 (UbcH5b,  $2.5~\mu M$ ), and the E3 ligase ( $0.2~or~0.4~\mu M$  of DDB1-CUL4A-RBX1 complexed with the various DCAF1 constructs as indicated) were incubated at 37 °C with  $0.5~\mu M$  of NusA-Vpr- $\Delta C$  (residue of 1–79), 1  $\mu M$  of UNG2, and  $2.5~\mu M$  of His $_6$ -FLAG-tagged ubiquitin in a buffer containing 10 mM TrisHCl, pH 7.5, 150 mM NaCl, 5% glycerol, 20 U/mL pyrophosphatase, 2 mM DTT, and 5 mM ATP for various lengths of time. Reactions were stopped by heating the samples in SDS-Laemmli buffer at 95 °C for 5 min. The extent of ubiquitination was determined by immunoblotting with anti-FLAG or anti-UNG2 (Abnova) antibodies, after separation of the reaction mixtures on 4–20% gradient SDS-PAGE, and transfer to nitrocellulose.

#### **Results and Discussion**

#### DCAF1 Proteins Oligomerize when ectopically expressed in insect cells

It is known that several CRLs dimerize via substrate receptor proteins (18,40–42,50). In addition, the DCAF1 sequence contains a Lissencephaly type 1-like homology motif (LisH) (51) between residues 846 and 876, known to mediate dimerization. It therefore seemed prudent to evaluate whether oligomerization of DCAF1 may occur, especially since during protein expression and purification of a long DCAF1 construct (residues 96–1507) aggregation was observed, with DDB1–DCAF1 complexes eluting in the void volume of a Superdex200 gel-filtration column (Ahn et al., unpublished results). The apparent discrepancy between the expected molecular mass (280 kD) of the complex and the experimental behavior warranted further examination.

In order to assess whether oligomerization of DCAF1 occurred, co-immunoprecipitation of transiently expressed, differentially tagged DCAF1 proteins in insect cells was carried out. Specifically, both N-terminally Myc-tagged DCAF1 and N-terminally FLAG-tagged DCAF1 (residue 96–1507) were transiently co-expressed in SF9 cells, with both constructs containing a V5-tag at their C-termini. Cell lysates were subjected to immunoprecipitation with anti-FLAG antibodies and indeed, interaction between the Myc-tagged and FLAG-tagged DCAF1 proteins was observed (Fig. 1A, lane 1).

The oligomerization domain was mapped by co-expressing various truncated DCAF1 constructs (residues 572–1507, 817–1507, 876–1396, 987–1396, and 1005–1507), tagged with the V5 epitope at their C-termini together with the FLAG-tagged DCAF1 (residues 96–1507). Immunoprecipitation with anti-FLAG antibodies, and subsequent immunoblotting with anti-V5 antibodies of co-expressed DCAF constructs revealed that the putative LisH motif, comprising residues 846–876, needed to be present for stable interaction (Fig. 1B). In particular, the 876–1396, 987–1396, or 1005–1507 constructs failed to co-immunoprecipitate with the FLAG-tagged DCAF1 96–1507 bait, while 572–1507 or 817–1407 constructs did. This data provided strong evidence for a possible direct interaction between DCAF1 proteins, mediated by residues 817–876 that contain the putative LisH motif. However, association of DCAF1 proteins via other endogenous cellular proteins could not be ruled out. To directly confirm the homo-oligomerization of DCAF1 proteins, the isolated peptide region implicated in the association was investigated as described below.

#### Secondary Structure of a DCAF1-LisH Peptide in Solution

The secondary structure of the LisH motif containing region of DCAF1 was investigated by NMR. Three different lengths of peptides were prepared, DCAF1 809–876, DCAF1 809–902 and DCAF1 841–883 (Fig. 2). Qualitative structural characterization of the DCAF1 809–876 WT peptide analyzing secondary chemical shifts ( $\Delta\delta C_{\alpha}$ – $\Delta\delta C_{\beta}$ ) clearly suggested that the C-terminal half of the peptide (Phe845–Glu873) exhibited an alpha helical conformation, indicated by a stretch of large positive values of secondary chemical shifts for Glu847–Ser860 and Leu862–Glu873, with a break at Lys861 (Fig. 2A). Most of the residues in the N-terminal half of DCAF1 809–876 also exhibit positive secondary chemical shifts, albeit too small to suggest that a helical structure is present. In order to unambiguously delineate the helix boundaries, the peptide was extended at its C-terminus up to residue 902 (Fig. 2B). The secondary chemical shifts for this longer peptide revealed that the helix terminates at Glu873. Further, a shorter DCAF1 peptide (residues 841–883) also displays similar boundaries for the helical region (Fig. 2C). This data confirms that the putative LisH motif (residues 846–876) is embedded in an alpha helical structure, in agreement with the well-characterized helical LisH motif of LIS1(52,53). One notable different feature of the

region surrounding the LisH motif in DCAF1 is that the residues following the motif display random coil properties. The canonical LisH motif is often followed by an extended coiled-coil segment with a short helical segment connecting these two regions (52,53). However, these coiled-coil segments do not contribute to dimerization and exhibit random coil properties as isolated fragments (53).

### The Region of the Four Leu Repeat is Essential for Alpha-helical Structure and Oligomerization of DCAF1

The LisH motif is present in numerous eukaryotic proteins, frequently N-terminal to WD40 domains (51), and in DCAF1 the prototypical L-X<sub>2</sub>-L-X<sub>3-5</sub>-L-X<sub>3-5</sub>-L sequence (51) is located at position 850–863. Sequence alignment of the pertinent DCAF1 region with orthologous sequences and human LIS1 is provided in Fig. 3A. Interestingly, the LisH motif of DCAF1 contains four Leu residues adjacent to Ile854, the residue that corresponds to the critical Ile15 residue in the dimer interface of the LIS1 structure (52,54). In order to assess whether these Leu residues are important for oligomer formation, we constructed two mutants of DCAF1, ΔN-L850E/L851E DCAF1-V5 (residues 817–1507 of L850E/L851E DCAF1 with a C-terminal V5-tag; 1LL/EE) and ΔN-L852E/L853E DCAF1-V5 (residues 817–1507 of L852E/L853E DCAF1 with a C-terminal V5-tag; 2LL/EE). Co-expression of either mutant with N-terminally FLAG-tagged and C-terminally V5-tagged DCAF1 (FLAG-DCAF1-V5, residues 96–1507) did not result in efficient co-immunoprecipitation (Fig. 3B, lane 2 and 4). In contrast, WT ΔN-DCAF1-V5 co-precipitated efficiently with FLAG-DCAF1-V5 (Fig. 3B, lane 1). This data suggests that residues within the Leu850–Leu853 stretch are essential for the interaction between different DCAF1 molecules.

To directly confirm that the four Leu-repeat in the LisH motif of DCAF1 is responsible for oligomerization, both mutations, 1LL/EE and 2LL/EE, were introduced into a Trx-peptide fusion construct and fusion proteins and the DCAF1 809-876 peptide were purified to homogeneity (Fig 3C). The quaternary states of Trx-DCAF1 809-876, Trx-DCAF1 809-876 1LL/EE, and Trx-DCAF1 809-876 2LL/EE were analyzed by a multi-angle light scattering. The experimental molecular mass of Trx-DCAF1 809-876 was derived as 51 kDa, significantly higher than the monomeric theoretical molecular mass (27 kDa) by almost twofold (Fig. 3D, ▼). The estimated molecular masses of the Trx-DCAF1 1LL/EE and 2LL/EE proteins were 33 kDa and 28 kDa, respectively, close to the theoretical monomer molecular masses (Fig. 3D, ♦ and • , respectively). For comparison, the unfused Trx protein eluted as a monomer, (experimental and theoretical molecular mass of ~18 kDa, ■). These light scattering data strongly suggest that indeed the LisH motif of DCAF1 is responsible for oligomerization, with the Leu repeat providing critical determinants at the interface. To monitor potential structural changes in the LisH motif upon Leu residue mutation, the Trx-DCAF1 809-876 WT, 1LL/EE, and 2LL/EE fusion proteins were cleaved with TEV protease and DCAF1 peptides purified (Fig. 4A, insert). The circular dichroism (CD) spectrum of the cleaved DCAF1 809-876 WT peptide exhibited two minima at 208 nm and 222 nm, indicating the presence of alpha-helical structure (Fig. 4, circles). The monomeric DCAF1 LL/EE mutants, however, exhibited CD spectra characteristic of random coil structure (Fig. 4, triangles and squares), suggesting that the four Leu repeat is essential for helix formation. For other LisH motif containing genes, it has been reported that diseaserelated mutations in this motif that abrogate oligomerization, affect protein half-life and alter cellular localization (54,55). In the present case, WT DCAF1 and LL/EE mutants in transiently transfected HEK293 cells essentially exhibited the same half-life (data not shown).

#### The Adaptor-Receptor Complex, DDB1-DCAF1 Dimerizes via the DCAF1 Helical Domain

DDB1 is an adaptor protein that binds to the scaffolding protein complex, CUL4A-RBX1 and the substrate receptor, DCAF1, forming the E3 ubiquitin ligase. To evaluate the quaternary state of the adaptor-receptor complex, DDB1 complexes containing the 817–1507 DCAF1 constructs were purified and analyzed by light scattering (Fig. 5). The observed molecular mass (411 kDa) of this complex is twice its theoretical value, (DDB1, 130 kDa; DCAF1 817–1507, 81 kDa), lending further support to the finding that the region encompassing the LisH motif of DCAF1 mediates dimerization of the DDB1–DCAF1 complexes.

## Electron Microscopy (EM) and 2D Image Analysis Suggests a Dimeric CRL<sup>DCAF1</sup> Organization

For electron microscopy, we reconstituted the entire CRL4<sup>DCAF1</sup> E3 ubiquitin ligase complex from its four components. As evidenced by SDS-PAGE (Fig. 6A), the four individual proteins in the complex are present in equimolar amounts (CUL4A, 87 kDa; RBX1, 12 kDa; DDB1, 130 kDa; DCAF1 817–1507, 81 kDa) resulting in an overall molecular mass of the complex of 650 kDa by light scattering, confirming its dimeric quaternary state (Fig. 6B). However, some smaller species, possibly sub-complexes, are also observed upon 50 fold dilution to 50 nM concentration (necessary for EM analysis). The larger particles represent the intact complex (Fig. 6C). They are well separated from each other and appear to be homogeneous with similar sizes after uranyl acetate staining. From EM projection images, the estimated diameter of a sphere required for enclosing these large particles is about 180Å, significantly larger than what would be expected for a monomeric, 330kDa CRL4<sup>DCAF1</sup> particle. Classification of approximately 1,900 particle images by multivariant statistical analysis from the raw micrographs resulted in the class averages depicted in Fig. 6D. Near-mirror symmetries were observed for a few of the 2D class averages (Fig. 6D), suggesting the presence of a twofold axis in the particles. Therefore, the EM study of CRL4<sup>DCAF1</sup> particles agrees well with the biochemical analyses described above.

### Possible Roles of Dimerization of DCAF1 in Ubiquitin Ligase Activity of CRL4<sup>DCAF1-Vpr</sup>

Dimerization of the CUL4A-RING E3 ligase can impart functional advantages onto the ligase complex, such as permitting productive loading of different size and shape substrates for ubiquitination. Many other ubiquitin E3 ligases dimerize via substrate receptor proteins. For example, in some Skp1-Cdc53/Cul1-F-box (SCF) E3 ligases, a small dimerization domain (D-box) is located within the substrate receptor protein (56,57). It is believed that dimerization of CRLs imparts variability in the overall geometry of the complexes, permitting ubiquitination of substrates in *cis* as well as in *trans* (40–44).

The ubiquitination activities of monomeric and dimeric CRL4<sup>DCAF1</sup> E3 ligases were tested using DCAF1 817–1507 (dimeric) or DCAF1 1005–1507 (monomeric) constructs (Fig. 7A). Although it is not clear which cellular substrates are targeted by CRL4<sup>DCAF1</sup>, we previously demonstrated that uracil DNA glycosylase-2 (UNG2) becomes ubiquitinated via CRL4<sup>DCAF1</sup> in a Vpr-dependent manner (46). Ubiquitin transfer activity of dimeric CRL4<sup>DCAF1</sup> is more than twofold higher than that of a monomeric complex (Fig. 7B. compare lanes 2–4 with 6–8 and lanes 10–12 with 14–16), supporting the notion that dimerization of substrate recognition proteins allows for more efficient ubiquitin transfer. However, other possible reasons for the observed difference could also be related to the missing region between the LisH motif and the start of the WD40 domain in monomeric CRL4<sup>DCAF1</sup>.

Previous structural data of DDB1 have revealed that the relative orientation of CUL4A-binding domain is variable relative to the substrate receptor-binding domains, creating different distances between CUL4A-RBX1 and the substrate. (19–21). This also may facilitate ubiquitination of substrates, and dimerization of DCAF1 potentially could add further conformational variability. However, it should be noted that the LisH motif is not commonly present among putative DCAF substrate receptors (58) and further structural and biochemical studies are necessary to fully evaluate the conformational variability in these complexes.

#### **Conclusions**

DCAF1, initially identified as a HIV-1 Vpr binding protein (VprBP) and belonging to the large family of WD40 domain containing substrate receptors of CUL4-RING E3 ubiquitin ligases, forms an adaptor-receptor complex with DDB1. Although several of DCAF1's biological functions have been described, our understanding of its activity in proteasomal-degradation of target substrates still remains refractory. In this report, we demonstrate that a stretch of Leu residues in the LisH sequence motif is essential for oligomerization. The LisH motif is embedded in a region of ca 40 amino acids (~840–880) that possesses helical structure and is located N-terminal to the WD40 domain of DCAF1. This region is important for dimerization of the CRL4 complex and dimeric CRL4<sup>DCAF1</sup> appears to possess enhanced Vpr-mediated ubiquitin transfer activity, compared to its mutant monomeric counterpart.

#### **Acknowledgments**

This work was supported by the National Institutes of General Medical Sciences (NIH Grant P50GM082251 to A. M. G. and GM085043 to P. Z.).

We thank Dr. Teresa Brosenitsch for critical reading of the manuscript, and Thomas Vu and Mathieu Cuchanski for expert technical assistance. We also thank Dr. Jacek Skowronski for communication of unpublished results.

#### **Abbreviations**

Ub

LisH

	1
<b>E1</b>	Ubiquitin-activating enzyme
E2	Ubiquitin-conjugating enzyme
E3	Ubiquitin ligase
ATP	adenosine triphosphate
RING	really interesting new gene
CUL	cullin
CRL	cullin-RING ubiquitin ligase
DDB1	DNA-damage-binding protein 1
DCAF1	DDB1-CUL4A-Associated Factor 1
HIV-1	human immunodeficiency virus-1
Vpr	viral protein, regulatory
LIS1	lissencephaly associated gene 1

LIS 1 homology

ubiquitin

**CRL4** DDB1-culling4A-RING ubiquitin ligase

CRL4DCAF1 CRL4 in complex with DCAF1

**EM** electron microscopy

**SEC-MALS** size-exclusion column chromatography coupled to in-line multi-angle light

scattering

#### References

1. Goldstein G, Scheid M, Hammerling U, Schlesinger DH, Niall HD, Boyse EA. Isolation of a polypeptide that has lymphocyte-differentiating properties and is probably represented universally in living cells. Proc Natl Acad Sci USA. 1975; 72:11–15. [PubMed: 1078892]

- Ciechanover A, Finley D, Varshavsky A. Ubiquitin dependence of selective protein degradation demonstrated in the mammalian cell cycle mutant ts85. Cell. 1984; 37:57–66. [PubMed: 6327060]
- Ciechanover A, Finley D, Varshavsky A. The ubiquitin-mediated proteolytic pathway and mechanisms of energy-dependent intracellular protein degradation. J Cell Biochem. 1984; 24:27– 53. [PubMed: 6327743]
- 4. Hershko A, Ciechanover A. The ubiquitin system. Annu Rev Biochem. 1998; 67:425–479. [PubMed: 9759494]
- Pickart CM. Mechanisms underlying ubiquitination. Annu Rev Biochem. 2001; 70:503–533.
  [PubMed: 11395416]
- Hicke L. Protein regulation by monoubiquitin. Nat Rev Mol Cell Biol. 2001; 2:195–201. [PubMed: 11265249]
- Hough R, Pratt G, Rechsteiner M. Ubiquitin-lysozyme conjugates. Identification and characterization of an ATP-dependent protease from rabbit reticulocyte lysates. J Biol Chem. 1986; 261:2400–2408. [PubMed: 3003114]
- 8. Pickart CM, Fushman D. Polyubiquitin chains: polymeric protein signals. Curr Opin Chem Biol. 2004; 8:610–616. [PubMed: 15556404]
- 9. Liu F, Walters KJ. Multitasking with ubiquitin through multivalent interactions. Trends Biochem Sci. 2010; 35:352–360. [PubMed: 20181483]
- Hershko A, Heller H, Elias S, Ciechanover A. Components of ubiquitin-protein ligase system.
  Resolution, affinity purification, and role in protein breakdown. J Biol Chem. 1983; 258:8206–8214. [PubMed: 6305978]
- 11. Pickart CM, Rose IA. Ubiquitin carboxyl-terminal hydrolase acts on ubiquitin carboxyl-terminal amides. J Biol Chem. 1985; 260:7903–7910. [PubMed: 2989266]
- 12. Pickart CM, Rose IA. Functional heterogeneity of ubiquitin carrier proteins. J Biol Chem. 1985; 260:1573–1581. [PubMed: 2981864]
- 13. Petroski MD, Deshaies RJ. Function and regulation of cullin-RING ubiquitin ligases. Nat Rev Mol Cell Biol. 2005; 6:9–20. [PubMed: 15688063]
- Kamura T, Conrad MN, Yan Q, Conaway RC, Conaway JW. The Rbx1 subunit of SCF and VHL E3 ubiquitin ligase activates Rub1 modification of cullins Cdc53 and Cul2. Genes & Dev. 1999; 13:2928–2933. [PubMed: 10579999]
- 15. Tan P, Fuchs SY, Chen A, Wu K, Gomez C, Ronai Z, Pan ZQ. Recruitment of a ROC1-CUL1 ubiquitin ligase by Skp1 and HOS to catalyze the ubiquitination of I kappa B alpha. Mol Cell. 1999; 3:527–533. [PubMed: 10230406]
- Wang G, Yang J, Huibregtse JM. Functional domains of the Rsp5 ubiquitin-protein ligase. Mol Cell Biol. 1999; 19:342–352. [PubMed: 9858558]
- 17. Bosu DR, Kipreos ET. Cullin-RING ubiquitin ligases: global regulation and activation cycles. Cell Div. 2008; 3:7. [PubMed: 18282298]
- 18. Merlet J, Burger J, Gomes JE, Pintard L. Regulation of cullin-RING E3 ubiquitin-ligases by neddylation and dimerization. Cell Mol Life Sci. 2009; 66:1924–1938. [PubMed: 19194658]

19. Li T, Chen X, Garbutt KC, Zhou P, Zheng N. Structure of DDB1 in complex with a paramyxovirus V protein: viral hijack of a propeller cluster in ubiquitin ligase. Cell. 2006; 124:105–117. [PubMed: 16413485]

- 20. Angers S, Li T, Yi X, MacCoss MJ, Moon RT, Zheng N. Molecular architecture and assembly of the DDB1-CUL4A ubiquitin ligase machinery. Nature. 2006; 443:590–593. [PubMed: 16964240]
- Scrima A, Konickova R, Czyzewski BK, Kawasaki Y, Jeffrey PD, Groisman R, Nakatani Y, Iwai S, Pavletich NP, Thoma NH. Structural basis of UV DNA-damage recognition by the DDB1-DDB2 complex. Cell. 2008; 135:1213–1223. [PubMed: 19109893]
- 22. Groisman R, Polanowska J, Kuraoka I, Sawada J, Saijo M, Drapkin R, Kisselev AF, Tanaka K, Nakatani Y. The ubiquitin ligase activity in the DDB2 and CSA complexes is differentially regulated by the COP9 signalosome in response to DNA damage. Cell. 2003; 113:357–367. [PubMed: 12732143]
- 23. Kapetanaki MG, Guerrero-Santoro J, Bisi DC, Hsieh CL, Rapic-Otrin V, Levine AS. The DDB1-CUL4ADDB2 ubiquitin ligase is deficient in xeroderma pigmentosum group E and targets histone H2A at UV-damaged DNA sites. Proc Natl Acad Sci USA. 2006; 103:2588–2593. [PubMed: 16473935]
- 24. He YJ, McCall CM, Hu J, Zeng Y, Xiong Y. DDB1 functions as a linker to recruit receptor WD40 proteins to CUL4-ROC1 ubiquitin ligases. Genes & Dev. 2006; 20:2949–2954. [PubMed: 17079684]
- 25. Higa LA, Wu M, Ye T, Kobayashi R, Sun H, Zhang H. CUL4-DDB1 ubiquitin ligase interacts with multiple WD40-repeat proteins and regulates histone methylation. Nat Cell Biol. 2006; 8:1277–1283. [PubMed: 17041588]
- 26. Jin J, Arias EE, Chen J, Harper JW, Walter JC. A family of diverse Cul4-Ddb1-interacting proteins includes Cdt2, which is required for S phase destruction of the replication factor Cdt1. Mol Cell. 2006; 23:709–721. [PubMed: 16949367]
- 27. Higa LA, Zhang H. Stealing the spotlight: CUL4-DDB1 ubiquitin ligase docks WD40-repeat proteins to destroy. Cell Div. 2007; 2:5. [PubMed: 17280619]
- 28. Jackson S, Xiong Y. CRL4s: the CUL4-RING E3 ubiquitin ligases. Trends Biochem Sci. 2009; 34:562–570. [PubMed: 19818632]
- 29. Transy C, Margottin-Goguet F. HIV1 Vpr arrests the cell cycle by recruiting DCAF1/VprBP, a receptor of the Cul4-DDB1 ubiquitin ligase. Cell Cycle. 2009; 8:2489–2490. [PubMed: 19667756]
- 30. Le Rouzic E, Morel M, Ayinde D, Belaidouni N, Letienne J, Transy C, Margottin-Goguet F. Assembly with the Cul4A-DDB1DCAF1 ubiquitin ligase protects HIV-1 Vpr from proteasomal degradation. J Biol Chem. 2008; 283:21686–21692. [PubMed: 18524771]
- 31. Wen X, Duus KM, Friedrich TD, de Noronha CM. The HIV1 protein Vpr acts to promote G2 cell cycle arrest by engaging a DDB1 and Cullin4A-containing ubiquitin ligase complex using VprBP/DCAF1 as an adaptor. J Biol Chem. 2007; 282:27046–27057. [PubMed: 17620334]
- 32. Tan L, Ehrlich E, Yu XF. DDB1 and Cul4A are required for human immunodeficiency virus type 1 Vpr-induced G2 arrest. J Virol. 2007; 81:10822–10830. [PubMed: 17626091]
- 33. Le Rouzic E, Belaidouni N, Estrabaud E, Morel M, Rain JC, Transy C, Margottin-Goguet F. HIV1 Vpr arrests the cell cycle by recruiting DCAF1/VprBP, a receptor of the Cul4-DDB1 ubiquitin ligase. Cell Cycle. 2007:182–188. [PubMed: 17314515]
- 34. Hrecka K, Gierszewska M, Srivastava S, Kozaczkiewicz L, Swanson SK, Florens L, Washburn MP, Skowronski J. Lentiviral Vpr usurps Cul4-DDB1[VprBP] E3 ubiquitin ligase to modulate cell cycle. Proc Natl Acad Sci USA. 2007; 104:11778–11783. [PubMed: 17609381]
- 35. DeHart JL, Zimmerman ES, Ardon O, Monteiro-Filho CM, Arganaraz ER, Planelles V. HIV-1 Vpr activates the G2 checkpoint through manipulation of the ubiquitin proteasome system. Virol J. 2007; 4:57. [PubMed: 17559673]
- 36. Belzile JP, Duisit G, Rougeau N, Mercier J, Finzi A, Cohen EA. HIV-1 Vpr-mediated G2 arrest involves the DDB1-CUL4AVPRBP E3 ubiquitin ligase. PLoS Pathog. 2007; 3:e85. [PubMed: 17630831]
- 37. Belzile JP, Richard J, Rougeau N, Xiao Y, Cohen EA. HIV-1 Vpr Induces the K48-Linked Polyubiquitination and Proteasomal Degradation of Target Cellular Proteins To Activate ATR and Promote G2 Arrest. J Virol. 2010; 84:3320–3330. [PubMed: 20089662]

38. Saha A, Deshaies RJ. Multimodal activation of the ubiquitin ligase SCF by Nedd8 conjugation. Mol Cell. 2008; 32:21–31. [PubMed: 18851830]

- 39. Duda DM, Borg LA, Scott DC, Hunt HW, Hammel M, Schulman BA. Structural insights into NEDD8 activation of cullin-RING ligases: conformational control of conjugation. Cell. 2008; 134:995–1006. [PubMed: 18805092]
- 40. McMahon M, Thomas N, Itoh K, Yamamoto M, Hayes JD. Dimerization of substrate adaptors can facilitate cullin-mediated ubiquitylation of proteins by a "tethering" mechanism: a two-site interaction model for the Nrf2-Keap1 complex. J Biol Chem. 2006; 281:24756–24768. [PubMed: 16790436]
- 41. Hao B, Oehlmann S, Sowa ME, Harper JW, Pavletich NP. Structure of a Fbw7-Skp1-cyclin E complex: multisite-phosphorylated substrate recognition by SCF ubiquitin ligases. Mol Cell. 2007; 26:131–143. [PubMed: 17434132]
- 42. Welcker M, Clurman BE. Fbw7/hCDC4 dimerization regulates its substrate interactions. Cell Div. 2007; 2:7. [PubMed: 17298674]
- 43. Tang X, Orlicky S, Lin Z, Willems A, Neculai D, Ceccarelli D, Mercurio F, Shilton BH, Sicheri F, Tyers M. Suprafacial orientation of the SCFCdc4 dimer accommodates multiple geometries for substrate ubiquitination. Cell. 2007; 129:1165–1176. [PubMed: 17574027]
- 44. Li Y, Hao B. Structural basis of dimerization-dependent ubiquitination by the SCF(Fbx4) ubiquitin ligase. J Biol Chem. 2010; 285:13896–13906. [PubMed: 20181953]
- Ahn J, Byeon IJ, Byeon CH, Gronenborn AM. Insight into the structural basis of pro- and antiapoptotic p53 modulation by ASPP proteins. J Biol Chem. 2009; 284:13812–13822. [PubMed: 19246451]
- 46. Ahn J, Vu T, Novince Z, Guerrero-Santoro j, Rapic-Otrin V, Gronenborn A. HIV-1 Vpr loads uracil DNA glycosylase-2 onto DCAF1, a substrate recognition subunit of a cullin 4A-RING E3 ubiquitin ligase for proteasome-dependent degradation. J Biol Chem. 2010; 285:37333–37341. [PubMed: 20870715]
- 47. Wishart DS, Bigam CG, Holm A, Hodges RS, Sykes BD. 1H, 13C and 15N random coil NMR chemical shifts of the common amino acids. I. Investigations of nearest-neighbor effects. J Biomol NMR. 1995; 5:67–81. [PubMed: 7881273]
- 48. Spera S, Ikura M, Bax A. Measurement of the exchange rates of rapidly exchanging amide protons: application to the study of calmodulin and its complex with a myosin light chain kinase fragment. J Biomol NMR. 1991; 1:155–165. [PubMed: 1668721]
- 49. Ludtke SJ, Baldwin PR, Chiu W. EMAN: semiautomated software for high-resolution single-particle reconstructions. J Struct Biol. 1999; 128:82–97. [PubMed: 10600563]
- 50. Chew EH, Poobalasingam T, Hawkey CJ, Hagen T. Characterization of cullin-based E3 ubiquitin ligases in intact mammalian cells--evidence for cullin dimerization. Cell Signal. 2007; 19:1071–1080. [PubMed: 17254749]
- 51. Emes RD, Ponting CP. A new sequence motif linking lissencephaly, Treacher Collins and oral-facial-digital type 1 syndromes, microtubule dynamics and cell migration. Hum Mol Genet. 2001; 10:2813–2820. [PubMed: 11734546]
- 52. Kim MH, Cooper DR, Oleksy A, Devedjiev Y, Derewenda U, Reiner O, Otlewski J, Derewenda ZS. The structure of the N-terminal domain of the product of the lissencephaly gene Lis1 and its functional implications. Structure. 2004; 12:987–998. [PubMed: 15274919]
- 53. Mateja A, Cierpicki T, Paduch M, Derewenda ZS, Otlewski J. The dimerization mechanism of LIS1 and its implication for proteins containing the LisH motif. J Mol Biol. 2006; 357:621–631. [PubMed: 16445939]
- 54. Gerlitz G, Darhin E, Giorgio G, Franco B, Reiner O. Novel functional features of the Lis-H domain: role in protein dimerization, half-life and cellular localization. Cell Cycle. 2005; 4:1632–1640. [PubMed: 16258276]
- Boulton SJ, Brook A, Staehling-Hampton K, Heitzler P, Dyson N. A role for Ebi in neuronal cell cycle control. EMBO J. 2000; 19:5376–5386. [PubMed: 11032805]
- 56. Wolf DA, McKeon F, Jackson PK. F-box/WD-repeat proteins pop1p and Sud1p/Pop2p form complexes that bind and direct the proteolysis of cdc18p. Curr Biol. 1999; 9:373–376. [PubMed: 10209119]

57. Suzuki H, Chiba T, Suzuki T, Fujita T, Ikenoue T, Omata M, Furuichi K, Shikama H, Tanaka K. Homodimer of two F-box proteins betaTrCP1 or betaTrCP2 binds to IkappaBalpha for signal-dependent ubiquitination. J Biol Chem. 2000; 275:2877–2884. [PubMed: 10644755]

58. Lee J, Zhou P. DCAFs, the missing link of the CUL4-DDB1 ubiquitin ligase. Mol Cell. 2007; 26:775–780. [PubMed: 17588513]

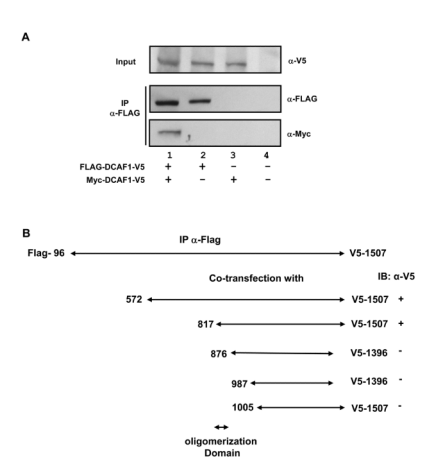


Figure 1. DCAF1 oligomerizes via a putative LisH motif IN VIVO

A. N-terminally FLAG-tagged and C-terminally V5-tagged DCAF1 (FLAG-DCAF1-V5, residues 96–1507) was transiently co-expressed with N-terminally Myc-tagged and C-terminally V5-tagged DCAF1 (Myc-DCAF1-V5, residues 96–1507) in SF9 insect cells. Cell lysates were immunoprecipitated with anti-FLAG agarose affinity gel, and pull-down mixtures were analyzed by immunoblotting with anti-FLAG and anti-Myc antibodies (IP), after separation by SDS-PAGE and transfer to nitrocellulose. 5% of total cell lysates were also immunoblotted with anti-V5 antibody (Input). B. FLAG-DCAF1-V5 was transiently co-expressed in SF9 cells with several deletion constructs of DCAF1 (residues 572–1507, 817–1507, 876–1396, 987–1396, and 1005–1507), containing the V5-tag at their C-termini. Each cell lysate was subjected to immunoprecipitation with anti-FLAG agarose affinity gel, and pull-down mixtures were analyzed by immunoblotting with anti-V5 antibody. Constructs pulled-down by FLAG-DCAF1-V5 are labeled by (+), and those not pulled down by (-).

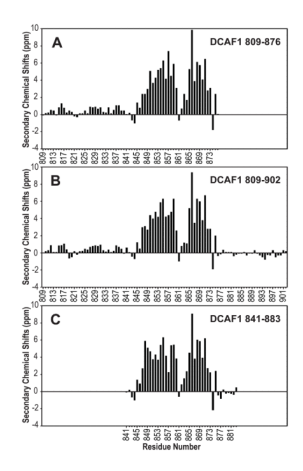
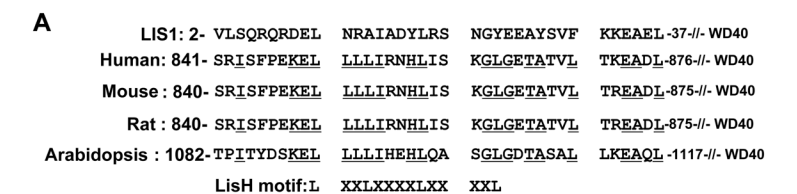
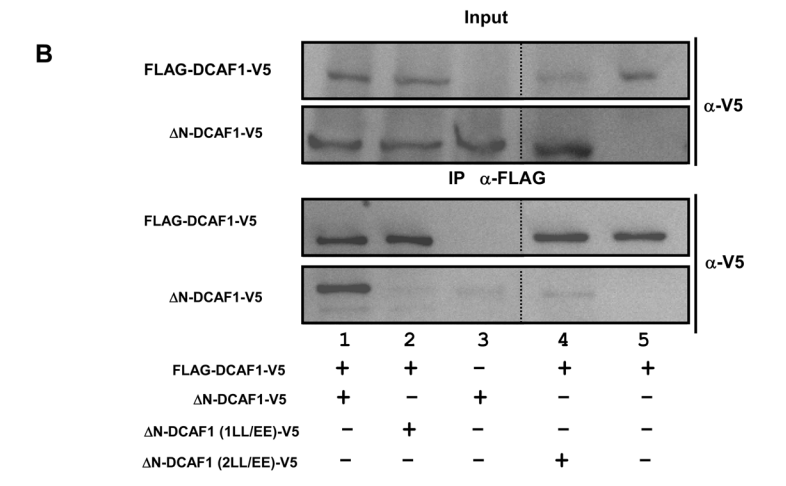


Figure 2. Secondary structure characterization of isolated DCAF1 peptides by NMR A–C, Secondary chemical shifts,  $\Delta C_{\alpha}$  minus  $\Delta C_{\beta}$ , (48) for DCAF1 809–876 (A), 809–902 (B) and 841–883 (C) are shown along the amino acid sequence.  $\Delta C_{\alpha}$  and  $\Delta C_{\beta}$  values were calculated for all assigned resonances by subtracting measured  $C_{\alpha}$  and  $C_{\beta}$  shifts from random coil values (47).





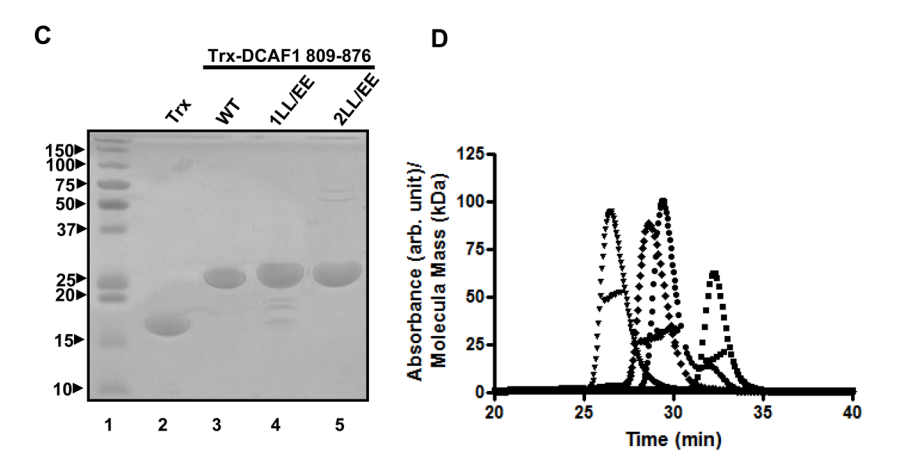


Figure 3. The four Leu region is critical for oligomerization of DCAF1

A. Sequence alignment of putative LisH domains in orthologous DCAF1s. Identical amino acid residues are underlined and the LisH motif, L-X<sub>2</sub>-L-X<sub>3-5</sub>-L-X<sub>3-5</sub>-L is displayed at the bottom. X represents any amino acid. B. FLAG-DCAF1-V5 (encoding residues of 96–1507) was transiently co-expressed with the N-terminally deleted DCAF1 (ΔN-DCAF1-V5, residues of 817–1507), site-directed mutants ΔN-DCAF1 (1LL/EE)-V5, and ΔN-DCAF1 (2LL/EE)-V5, respectively. 1LL/EE corresponds to the Leu850Glu, Leu851Glu double mutant, and 2LL/EE to the Leu852Glu, Leu853Glu double mutant. Cell lysates were immunoprecipitated with anti-FLAG agarose affinity gel. Proteins bound to antibodies were separated by SDS-PAGE, and subjected to immunoblotting with anti-V5 antibody after transfer to nitrocellulose. C. The DCAF1 region corresponding to residues 809–876 and the 1LL/EE and 2LL/EE mutants thereof were expressed and purified from *E. coli* as thioredoxin (Trx) fusion proteins. Trx and the three Trx-DCAF1 proteins were separated by SDS-PAGE and stained with Coomassie Brillant Blue. D. Multi-angle light scattering of purified Trx-DCAF1 fusion proteins and Trx as a control. Each protein (ca. 2 mg/mL) was

injected into an analytical Superdex200 gel filtration column at a flow rate of 0.5 mL/min. The UV (A<sub>280</sub>) elution profiles of Trx-DCAF1 809–876 WT ( $\blacktriangledown$ ), Trx-DCAF1 809–876 1LL/EE ( $\bullet$ ), Trx-DCAF1 809–876 2LL/EE ( $\bullet$ ), and Trx ( $\blacksquare$ ) are shown. The estimated molecular masses from the scattering data are shown across the elution peaks.

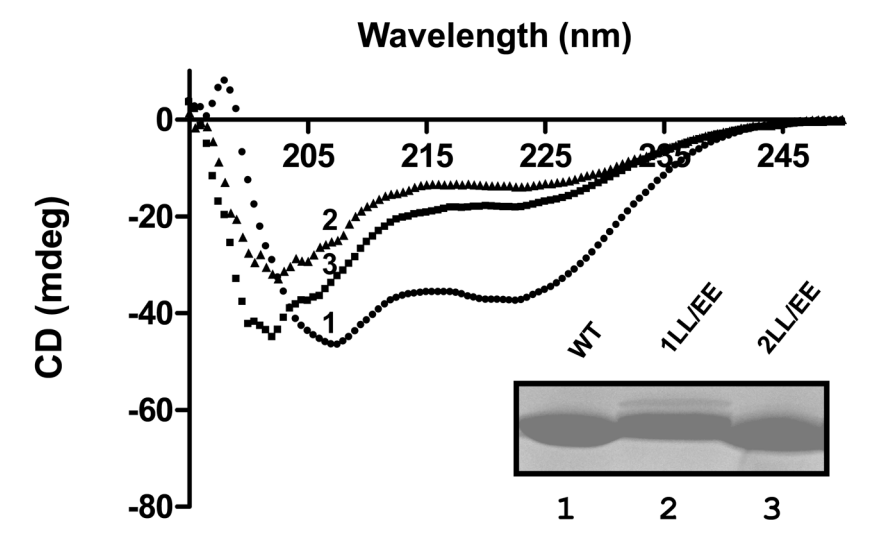


Figure 4. Secondary structure characterization of WT and mutant LisH motif peptides by CD Circular Dichroism (CD) spectra of WT DCAF1 809–876 (1,  $\bullet$ ), 1LL/EE 809–876 (2,  $\blacktriangle$ ), and 2LL/EE 809–876 (3,  $\blacksquare$ ), recorded at 3.3  $\mu$ M in a buffer containing 2.5 mM sodium phosphate, pH 7.5, 15 mM NaCl, at 25 °C. Data were collected at 0.5 nm intervals, scanned from 250–195 nm, and averaged over 10 measurements. The inset shows the SDS-PAGE analysis of the peptides used for CD.

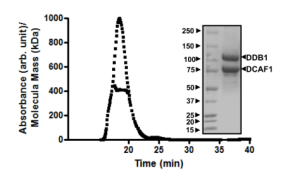


Figure 5. Characterization of the DDB1-DCAF1 complex by SEC-MALS and SDS-PAGE The DDB1-DCAF1 817–1507 protein complex was injected into an analytical gel filtration column at a flow rate of 0.5 mL/min. The UV ( $A_{280}$ ) elution profile and the estimated molecular mass from the scattering data are shown across the elution peaks. The protein complex was separated by SDS-PAGE and proteins visualized by Coomassie Brillant Blue.

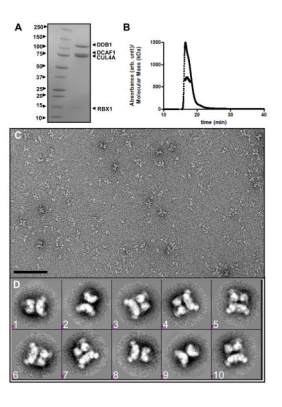
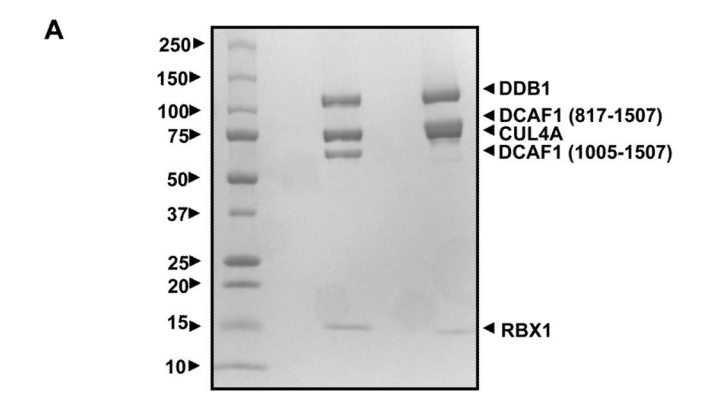


Figure 6. Electron microscopy of  $CRL4^{DCAF1}$  E3 ligase complexes A. SDS-PAGE analysis of the  $CRL4^{DCAF1}$  E3 ligase complex, assembled with CUL4A, RBX1, DDB1, and DCAF1 (residues 817–1507). Each component of the complex is indicated. B. SEC-MALS analysis of the CRL4DCAF1 E3 ligase complex. The protein complex was injected into an analytical gel filtration column at a flow rate of 0.5 mL/min and the data were analyzed as described in Experimental Procedures. The estimated molecular mass is shown across the elution peak. C. Electron micrograph of negatively stained CRL4DCAF1 complexes (scale bar, 100 nm). D. Selected 2D class averages of CRL4<sup>DCAF1</sup> complex particles selected from the micrograph. Some class averages show near mirror symmetry suggesting the presence of a 2-fold axis in the complexes.



В

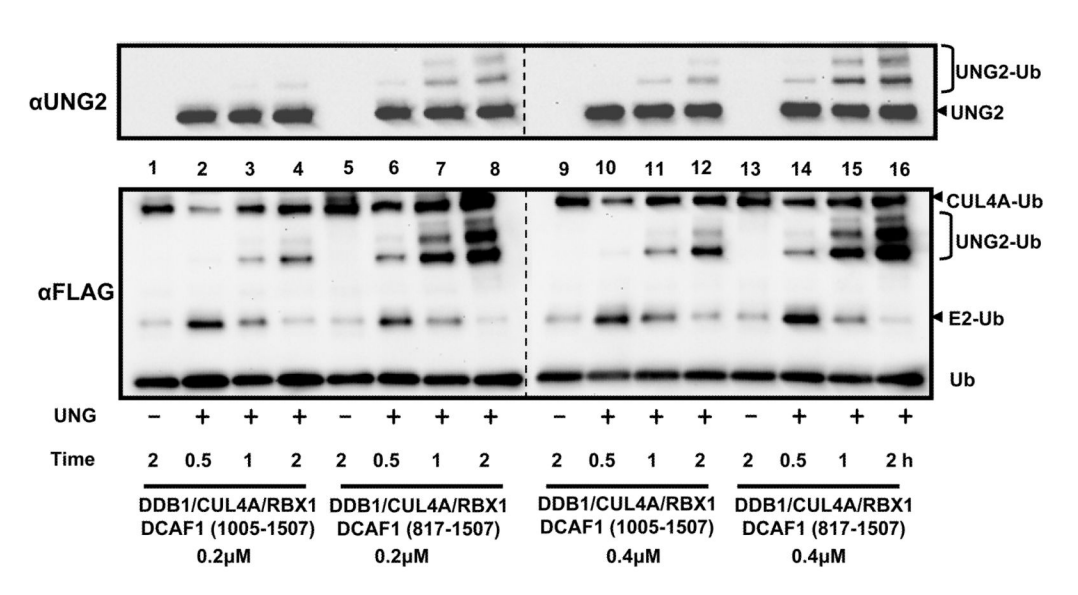


Figure 7. Ubiquitination activity of monomeric and dimeric CRL4<sup>DCAF1</sup> A. 20 pmol of monomeric CRL4 complex bound to DCAF1 (1005–1507) and dimeric CRL4 bound to DCAF1 (817–1507) separated by SDS-PAGE and visualized with Coomassie Blue. B. Time course of UNG2 ubiquitination with dimeric CRL4<sup>DCAF1</sup> and monomeric CRL4<sup>DCAF1</sup> at two different concentrations (0.2 and 0.4  $\mu$ M). The reaction buffer contained E1 (UBA1), E2 (UbcH5b), FLAG-tagged ubiquitin (Ub), and NusA-Vpr- $\Delta$ C. Ubiquitinated proteins were detected by immunoblotting with either anti-UNG2 or anti-FLAG antibody after separation of the reaction mixture on SDS-PAGE and transfer to nitrocellulose.